

# DISCOVERY OF RECENT STAR FORMATION IN THE EXTREME OUTER REGIONS OF DISK GALAXIES

Annette M. N. Ferguson<sup>1,2,3</sup> and Rosemary F.G. Wyse<sup>2,3</sup>

Department of Physics and Astronomy, The Johns Hopkins University, Baltimore, MD 21218

J. S. Gallagher

Department of Astronomy, University of Wisconsin, Madison, WI 53706

Deidre A. Hunter

Lowell Observatory, 1400 W. Mars Hill Road, Flagstaff, AZ 86001

## ABSTRACT

We present deep H $\alpha$  images of three nearby late-type spiral galaxies (NGC 628, NGC 1058 and NGC 6946), which reveal the presence of HII regions out to, and beyond, two optical radii (defined by the 25th B-band isophote). The outermost HII regions appear small, faint and isolated, compared to their inner disk counterparts, and are distributed in organized spiral arm structures, likely associated with underlying HI arms and faint stellar arms. The relationship between the azimuthally-averaged H $\alpha$  surface brightness (proportional to star formation rate per unit area) and the total gas surface density is observed to steepen considerably at low gas surface densities. We find that this effect is largely driven by a sharp decrease in the covering factor of star formation at large radii, and not by changes in the rate at which stars form locally. An azimuthally-averaged analysis of the gravitational stability of the disk of NGC 6946 reveals that while the existence of star formation in the extreme outer disk is consistent with the Toomre- $Q$  instability model, the low rates observed are only compatible with the model when a constant gaseous velocity dispersion is assumed. We suggest that observed behaviour could also be explained by a model in which the star formation rate has an intrinsic dependence on the azimuthally-averaged gas *volume* density, which decreases rapidly in the outer disk due to the vertical flaring of the gas layer.

*Subject headings:* galaxies: evolution – galaxies: individual (NGC 628, NGC 1058, NGC 6946) – HII regions – stars: formation

---

<sup>1</sup> Current Address: Institute of Astronomy, University of Cambridge, Madingley Road, Cambridge, UK CB3 0HA

<sup>2</sup>Visiting Astronomer, Kitt Peak National Observatory. KPNO is operated by AURA, Inc. under contract to the National Science Foundation.

<sup>3</sup>Visiting Astronomer, Lowell Observatory.

## 1. Introduction

An understanding of the processes which drive large-scale star formation in galactic disks is of great importance for models of disk formation and evolution. The present-day star formation rates in the previously poorly explored, faint outer regions of disks (i.e.  $R \gtrsim R_{25}$ , where  $R_{25}$  is defined by the 25th magnitude B-band isophote) provide important and unique insight on the nature of the star formation law in disk galaxies. Competing models make definite and distinct predictions for the expected behavior in these parts (eg. Prantzos & Aubert 1995, Tosi 1996). Characterized by their low gas surface densities (yet high gas fractions), low metallicities and long dynamical timescales, these outer regions provide a probe of star formation in physical environments which are very different from those typical of the bright, inner regions of disks, but are similar to those inferred for many high-redshift damped Lyman- $\alpha$  systems, (eg. Pettini et al 1997), as well as giant low surface brightness galaxies (eg. Pickering et al 1997).

In order to investigate the past and present star formation rates in the extreme outer regions of disks, we have obtained wide field-of-view (FOV), deep H $\alpha$  and broadband images for a sample of  $\sim 20$  nearby disk galaxies. In this Letter, we present first H $\alpha$  results for 3 galaxies (NGC 628 (D=10.7 Mpc), NGC 1058 (D=10.0 Mpc), NGC 6946 (D=5.3 Mpc)) where we have discovered HII regions, hence recent massive star formation, at particularly large radii. These late-type spirals are all characterized by larger than average HI-to-optical sizes. The results and interpretation from the full sample will be presented in Ferguson et al (1998a,b). Chemical abundance measurements for several of our newly-discovered outer-disk HII regions are presented in Ferguson et al (1998c).

## 2. Observations and Data Analysis

Wide-field CCD observations were obtained for our galaxies using the KPNO 0.9 m (NGC 628, NGC 6946) and the Lowell 1.8 m (NGC 1058). At KPNO, we used the Tek 2048x2048 CCD at the f/7.5 Cassegrain focus, with a FOV of  $23' \times 23'$ , and  $0.69''/\text{pixel}$ . At Lowell, we used the TI 800x800 CCD with the Ohio-State Imaging Fabry-Perot Spectrometer as 5:1 focal reducer, providing a FOV  $\sim 7'$  on a side, with  $0.49''/\text{pixel}$ . Image reduction was carried out in the standard manner (see Ferguson et al 1996). The radial variation of azimuthally-averaged H $\alpha$  surface brightness was determined using elliptical aperture photometry on the H $\alpha$  images. It was possible to do surface photometry on our images only out to approximately  $R_{25}$ , at which point errors in the background dominated the signal and often conspired to produce negative total fluxes in a given annulus despite the fact that HII regions (albeit faint) would be clearly visible on our images. To circumvent this problem, we counted emission only above a local isophotal threshold. This approach was equivalent to carrying out areal surface photometry in the inner disk, where the covering fraction of emission above our threshold surface brightness was high, and to carrying out photometry of discrete HII regions in the far outer disk. The typical threshold employed, always several times larger than the large-scale flat-field error, was  $\sim 3 \times 10^{-17} \text{ erg s}^{-1} \text{ cm}^{-2} / \square''$ , which

is considerably lower than those usually used to define the boundaries of discrete HII regions (e.g. Kennicutt 1988; Feinstein 1997) and also lower than the typical surface brightnesses exhibited by bright-moderate diffuse ionized gas (eg. Ferguson et al 1996). This method of counting pixels only where there is clearly emission allows us to get around the limitations imposed by the flat-field errors, but it should be kept in mind that it provides *strictly a lower limit* to the mean H $\alpha$  surface brightness in each annulus. A full discussion of the analysis will be included in Ferguson et al (1998a).

H $\alpha$  continuum-subtracted images for the galaxies are shown in Figure 1.

### 3. Discovery of Recent Star Formation in the Extreme Outer Limits of Disks

An exciting and unexpected result is the discovery of recent massive star formation in the extreme outer limits of all three galaxies. While early photographic studies of two of them revealed the existence of HII regions out to slightly beyond the optical radius (eg. Hodge 1969, Bonnarel et al 1986), our data indicate the presence of HII regions out to the extent of our imagery, i.e. to more than two optical radii.

Our images show a striking difference between the inner and outer disk HII regions, in that star formation the outer disk occurs in smaller, fainter and more isolated HII regions. The brightest outer disk HII regions detected here have diameters of 150–500 pc and H $\alpha$  luminosities of only 1–80  $\times 10^{37}$  erg s $^{-1}$ . Assuming that the HII regions are ionization-bounded (which may well not be the case, e.g. Ferguson et al 1996) and that they have negligible internal extinction (see Ferguson et al 1998c), the stellar Lyman continuum fluxes from Vacca et al (1996) predict a typical (lower limit to the) ionizing population of 0.2–20 equivalent O5V stars. Establishing whether the populations of inner and outer disk HII regions are indeed intrinsically different, or this merely reflects poor statistical sampling of the HII region luminosity function in the outer disk, will be a difficult, yet important, task.

The degree of organization of the outer disk star formation is also remarkable. The outer HII regions are not randomly distributed, but rather are in long, narrow spiral arms, more obviously in NGC 628 and NGC 6946. Our deep broad-band images reveal the existence of faint ( $B \sim 26\text{--}28$  mag/ $\square''$ ) stellar arms in all three galaxies, associated with these HII arms (Ferguson et al 1998a). Furthermore, inspection of published HI maps also reveals outer spiral arms in the underlying neutral gas (eg. Shostak & van der Kruit 1984; Dickey et al 1990; Kamphuis 1993). The relationship between the inner and outer spiral structure remains unclear, as indeed is the dynamics underlying the outer arms. The lack of obvious companions to any of these galaxies makes the tidal hypothesis for spiral arm formation unlikely; future observations in the near-IR will help to distinguish between alternative theories for the outer spiral patterns, such as long-lived density waves, or transient shearing perturbations.

The existence of massive stars in the extreme outer regions of disks means that stellar

feedback is also active in these parts. The typical outer disk star formation rates are  $\sim 0.01\text{--}0.05 M_{\odot} \text{ pc}^{-2} \text{ Gyr}^{-1}$ , giving Type II supernova rates of  $\sim 1\text{--}4 \times 10^{-4} \text{ SN pc}^{-2} \text{ Gyr}^{-1}$  (assuming a Salpeter IMF, with  $0.1 M_{\odot} \lesssim M \lesssim 100 M_{\odot}$ , and that all stars with  $M \gtrsim 8 M_{\odot}$  explode as supernovae). Reasonable estimates of their coupling efficiency to the ISM suggest that massive stars are likely to play a significant role in the energy balance of the outer disk (but not in supporting the HI velocity dispersion; Sellwood and Balbus 1998).

## 4. Discussion

### 4.1. The Rate of Star Formation in Outer Galactic Disks

The radial behaviour of the azimuthally-averaged  $H\alpha$  surface brightness distribution ( $\Sigma_{H\alpha}$ ) traces the mean massive-star formation rate per unit area across the disk. Figure 2 (left panel) presents the deprojected (corrected for  $\cos i$ ), azimuthally-averaged radial profiles of  $\Sigma_{H\alpha}$ , as derived above. These profiles are corrected for [NII] contamination and Galactic extinction, but not for extinction within the galaxies themselves. Figure 2 (right panel) shows the relationship between the azimuthally-averaged total gas surface density (atomic plus molecular gas with corrections for heavy elements) and the  $H\alpha$  profiles.

The azimuthally-averaged  $H\alpha$  surface brightness declines with increasing radius, but with evidence for a change in the behavior of the gradient in the outer disk, in all galaxies. The surface brightness profiles of NGC 628 and NGC 6946 both exhibit a sharp fall-off in  $\Sigma_{H\alpha}$  near the edge of the optical disk, with a subsequent flattening of the decline at larger radii. Steepenings are also seen at low gas column densities in plots of  $\Sigma_{H\alpha}\text{--}\Sigma_{gas}$ , where they occur at azimuthally-averaged total gas surface densities of  $5\text{--}10 M_{\odot}/\text{pc}^2$ , close to that estimated to be required to shield the molecular cloud cores from photodissociation by the ambient UV radiation field (eg. Federman et al 1979). Indeed the location of the steepenings is approximately coincident to the radius where the disk undergoes the transition from being dominated by (warm) molecular to atomic gas.

The existence of abrupt declines in the azimuthally-averaged  $H\alpha$  surface brightnesses, hence star formation rates, at low gas surface densities make it impossible to describe the observations with a single-component Schmidt law (Schmidt 1959), with a dependence on gas surface density alone. Plots of the mean HII region surface brightness in each annulus, which traces the mean star formation rate per unit area in regions where star formation is actually occurring, show only a modest variation with both radius and azimuthally-averaged gas surface density (see Figure 2). The abrupt steepenings observed in the azimuthally-averaged profiles must therefore be almost entirely due to sharp declines in the *covering factor* of star formation in the outer disk.

## 4.2. Does Gravitational Instability Drive Outer Disk Star Formation?

The large-scale star formation process in galaxies is intimately connected to the formation of gravitationally-bound gas complexes, and giant molecular clouds (eg. Larson 1992). The instability driving cloud formation may well be gravitational; in this case the Toomre- $Q$  criterion (Toomre 1964) yields a critical gas surface density above which one expects local instability to axisymmetric perturbations. For an infinitely thin, one component isothermal gas disk, the critical gas surface density above which self-gravity overcomes shear and pressure is given by

$$\Sigma_{crit} = \frac{\alpha\sigma\kappa}{\pi G} \quad (1)$$

where  $\alpha$  is a constant of order unity,  $\sigma$  is the velocity dispersion of the gas and  $\kappa$  is the epicyclic frequency<sup>4</sup>. Following Kennicutt (1989), we adopt  $\alpha = 0.67$ .

Published rotation curves and HI velocity dispersions exist for all three galaxies, and can be used to calculate the radial variation of  $\Sigma_{crit}$ . Both NGC 628 and NGC 1058 have very low inclinations however, which means that the amplitude and shape of their rotation curves are somewhat uncertain; for this reason, we will not consider them further here. For NGC 6946, we adopt the rotation curve of Sofue (1996), normalised using the inclination derived by Carignan et al (1990). We made two estimates of the critical gas surface density, one assuming a constant gas velocity dispersion ( $6 \text{ km s}^{-1}$ , for consistency with Kennicutt 1989) and the other including the radial variation determined directly from the HI observations (Kamphuis 1993). Figure 3 shows the radial variation of the ratio of the azimuthally-averaged, deprojected total gas surface density to the critical gas surface density, calculated for each case.

The ratio of the observed gas density to the estimated critical density is approximately constant across the range of radii probed by our observations (the maximum variation is only a factor of 2 over two optical radii). Considering the likely uncertainties in the input data which enter into the calculation – eg. rotation curves, velocity dispersions, gas surface densities (specifically the possible variation of the CO–H<sub>2</sub> conversion factor, and the existence of cold molecular gas) – this result is even more compelling.

When a constant velocity dispersion is assumed, NGC 6946’s disk should become stable exactly at the optical radius. The gas in the extreme outer disk hovers very near the instability limit out to two optical radii ( $\Sigma_{gas}/\Sigma_{crit} \sim 0.8-1$ , or  $1.5 \lesssim Q \lesssim 1.9$ ). The sharp decline in azimuthally-averaged star formation rate is observed to begin at  $0.8 R_{25}$ ; if this behavior is to be ascribed to a transition in the stability of the underlying gas disk, then either the value of  $\alpha$  or the velocity dispersion (or the combination) needs to be increased by approximately 20%. On the other hand, when the observed radial variation of the velocity dispersion is used in the calculation, we find that the disk hovers just below the instability limit at all radii ( $\Sigma_{gas}/\Sigma_{crit} \sim 0.7-0.9$ , or  $1.7 \lesssim Q \lesssim 2.1$ ). In this case, the inner and outer disks are indistinguishable in terms of their

---

<sup>4</sup>The epicyclic frequency is defined as  $\kappa = \sqrt{2} \frac{V}{R} \sqrt{1 + \frac{R}{V} \frac{dV}{dR}}$ .

local stability, and no critical radius can be defined; a  $Q$ -threshold therefore cannot provide an explanation for the steep declines in the covering factor of star formation observed in the outermost parts of the disk.

Our analysis for NGC 6946 suggests that the extreme outer disk probably lies close enough to the  $Q$ -stability limit so that processes such as swing amplification can operate and perhaps trigger star formation locally (eg. Larson 1992). While gravitational instability considerations may thus be able account for the existence of star formation at large radii, only the assumption of a constant gaseous velocity dispersion provides a basis for understanding the much reduced rates. The sizes of the star formation complexes and the spacing of the spiral arms may also be difficult to reconcile with the gravitational instability model, since the theoretically most unstable wavelength is much larger, and much smaller, respectively, than those features which are observed in the extreme outer disk (Ferguson et al 1998a).

### 4.3. Star Formation in Flaring Gas Disks

A possible alternative explanation for the observed behavior could be an intrinsic correlation between azimuthally-averaged star formation rate and gas *volume* density, combined with a vertical flaring of the gas disk, such that the transformation between gas surface density and volume density varies with galactocentric radius (see also Madore et al 1974). It is well known that gaseous disks exhibit an increase of scaleheight at large radius (eg. Merrifield 1992, Olling 1996). HII regions, however, are confined to a rather thin plane with a constant scaleheight (eg. Lockman, Pisano & Howard 1996). The combination of an increase in gas scale height with radius with the slow decline of gas surface density could conspire to produce a rapid decline in areal star formation rate between the inner and the outer disks. The magnitude of the flarings required to reproduce the behavior of the large-scale star formation rate do not appear unreasonable; a quantitative discussion is given in Ferguson et al (1998b).

We thank Jerry Sellwood, Rob Kennicutt and Jean-Rene Roy for interesting and useful discussions. This project was supported by an Amelia Earhart Fellowship from Zonta International (AMNF), NASA grant NAGW-2892 (RFGW) and NASA contract NAS 7-1260 to JPL (JSG).

### REFERENCES

- Bonnarel, F., Boulesteix, J. & Marcelin, M. 1986, A&AS, 66, 149  
Carignan, C., Charbonneau, P., Boulanger, F. & Viallefond, F. 1990, A&A, 234, 43  
Federman, S. R., Glassgold, A. E. & Kwan, J. 1979, ApJ, 227, 466  
Feinstein, C. 1997, ApJS, 112, 29

- Ferguson, A. M. N., Wyse, R. F. G., Gallagher, J. S. & Hunter, D. A. 1996, *AJ*, 111, 2265
- Ferguson, A. M. N., Wyse, R. F. G., Gallagher, J. S. & Hunter, D. A. 1998a, in preparation.
- Ferguson, A. M. N., Wyse, R. F. G., Gallagher, J. S. & Hunter, D. A. 1998b, in preparation.
- Ferguson, A. M. N., Gallagher, J. S. & Wyse, R. F. G. 1998c, *AJ*, August 1998 issue.
- Hodge, P. W. 1969, *ApJS*, 17, 467
- Kamphuis, J. 1993, Ph. D. Thesis, Groningen University
- Kennicutt, R. C. 1988, *ApJ*, 334, 144
- Kennicutt, R. C. 1989, *ApJ*, 344, 689
- Larson, R. B. 1992 in *Star Formation in Stellar Systems*, eds. G. Tenorio-Tagle, M. Prieto, & F. Sanchez (Cambridge University Press, Cambridge), p. 125
- Lockman, J. Pisano, D. J. & Howard, G. J. 1996, *ApJ*, 472, 173
- Madore, B. F., van den Bergh, S. & Rogstad, D. H. 1974, *ApJ*, 191, 317
- Merrifield, M. R. 1992, *AJ*, 103, 1552
- Olling, R. P. 1996, *AJ*, 112, 481
- Pettini, M., Smith, L. J., King, D. L. & Hunstead, R. W. 1997, *ApJ*, 486, 665
- Pickering, T., Impey, C., van Gorkom, J. & Bothun, G. 197, *AJ*, 114, 1858
- Prantzos, N. & Aubert, O. 1995, *A&A*, 302, 69
- Schmidt, M. 1959, *ApJ*, 129, 243
- Sellwood, J. A. & Balbus, S. A. 1998, *ApJ*, in press.
- Shostak, G. S. & van der Kruit, P. C. 1984, *A&A*, 132, 20
- Sofue, Y. 1996, *ApJ*, 458, 120
- Toomre, A. 1964, *ApJ*, 139, 1217
- Tosi, M. 1996 in *From Stars to Galaxies*, eds. C. Leitherer, U. Fritze-von Alvensleben & J. Huchra (Astronomical Society of the Pacific, San Francisco), p. 299
- Vacca, W. D., Garmany, C. D. & Shull, J. M. 1996, *ApJ*, 460, 914

Fig. 1a.—  $\text{H}\alpha + [\text{NII}]$  continuum-subtracted image of NGC 628; the optical radius ( $R_{25}$ ) is marked.

Fig. 1b.—  $\text{H}\alpha + [\text{NII}]$  continuum-subtracted image of NGC 1058; the optical radius ( $R_{25}$ ) is marked.

Fig. 1c.—  $\text{H}\alpha + [\text{NII}]$  continuum-subtracted image of NGC 6946; the optical radius ( $R_{25}$ ) is marked.



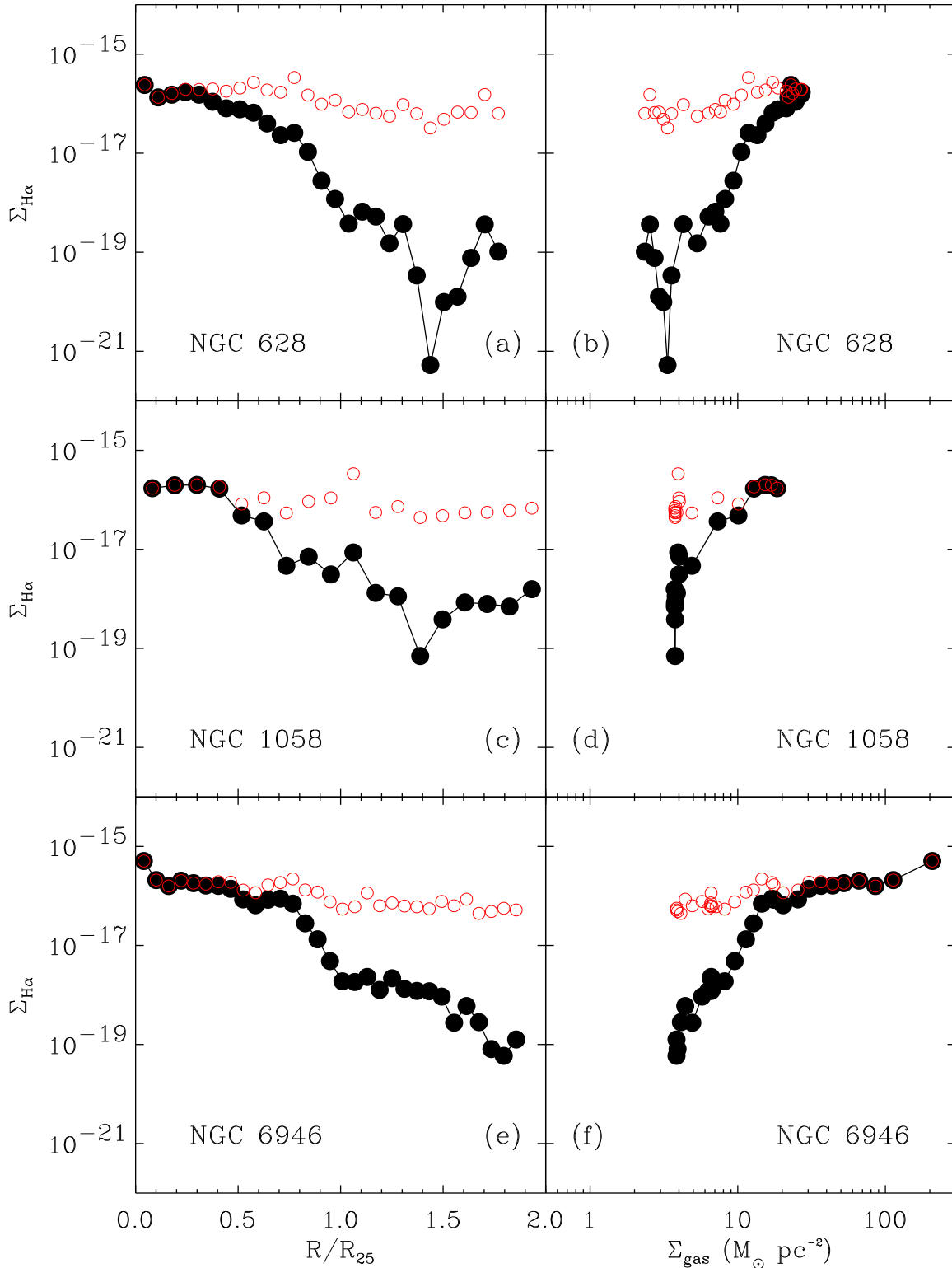


Fig. 2.— (Left panel) The radial variation of the deprojected, azimuthally-averaged H $\alpha$  surface brightness,  $\Sigma_{H\alpha}$  (in erg s $^{-1}$  cm $^{-2}$  /  $\square''$ ) as determined via elliptical aperture photometry (solid circles). (Right panel) The variation of  $\Sigma_{H\alpha}$  with the azimuthally-averaged total gas surface density,  $\Sigma_{gas}$ , where both quantities have been determined as a function of galactocentric radius in a series of elliptical annuli (solid circles). Also plotted are the mean HII region surface brightnesses, which

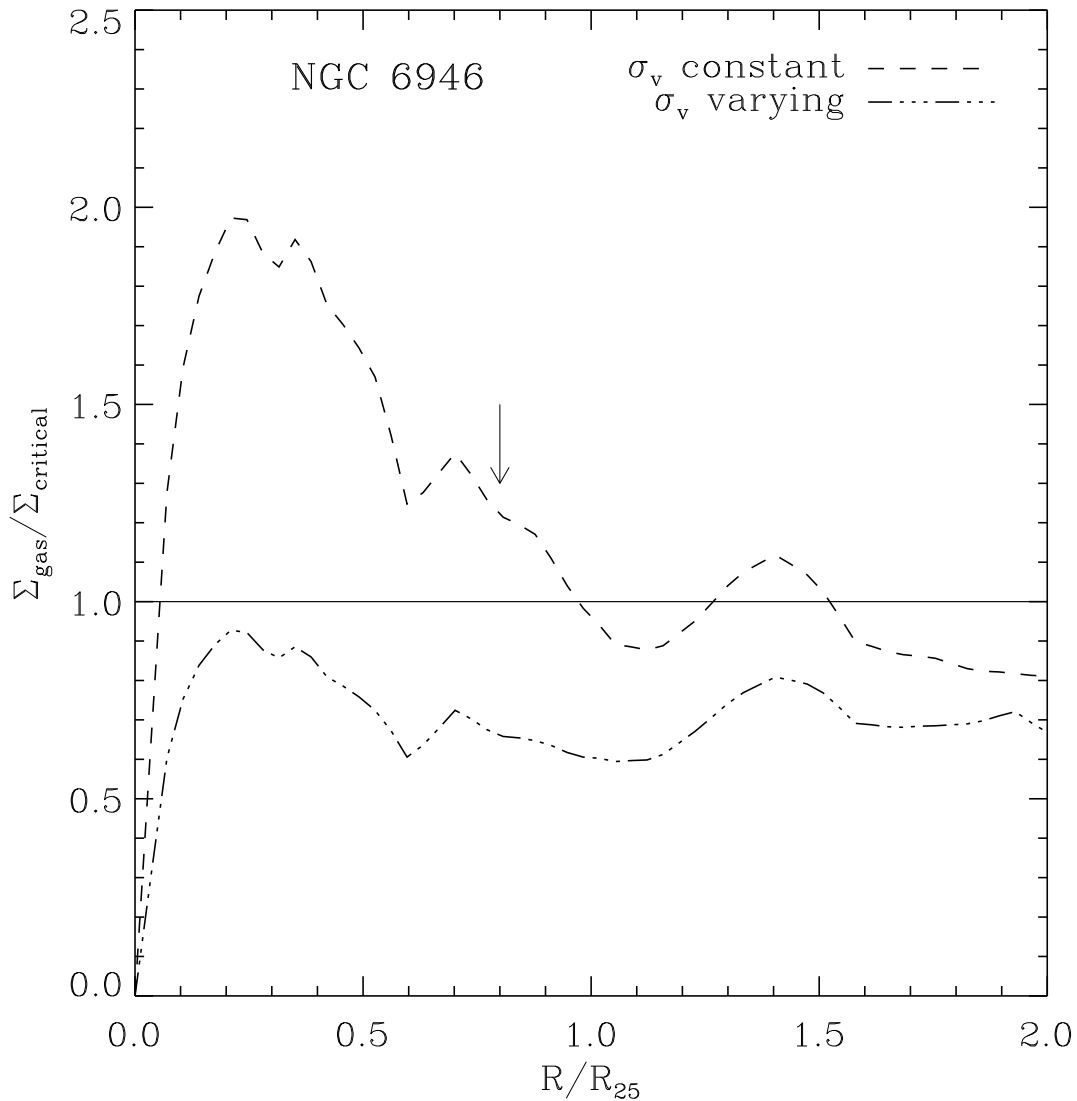


Fig. 3.— The radial variation of the ratio of the azimuthally-averaged (observed) gas surface density to the critical surface density for gravitational instability, calculated using both a constant velocity dispersion (dashed line) and a radially-varying one (dashed-dotted line). The solid horizontal line indicates the value of the ratio above which instability is expected. The small arrow indicates the point in the disk where the azimuthally-averaged star formation starts to decline sharply.

This figure "ferguson.fig1a.jpg" is available in "jpg" format from:

<http://arxiv.org/ps/astro-ph/9808151v1>

This figure "ferguson.fig1b.jpg" is available in "jpg" format from:

<http://arxiv.org/ps/astro-ph/9808151v1>

This figure "ferguson.fig1c.jpg" is available in "jpg" format from:

<http://arxiv.org/ps/astro-ph/9808151v1>